Experimental Study of the Effects of the Cathode Position and the Electrical Circuit Configuration on the Operation of HK40 Hall Thruster and BUSTLab Hollow Cathode

Nazli Turan,* Ugur Kokal,† Murat Celik‡

Bogazici University, Istanbul, 34342, Turkey

Huseyin Kurt§

Istanbul Medeniyet University, Istanbul, 34700, Turkey

HK40 Hall thruster, designed and developed at the Bogazici University Space Technologies Laboratory (BUSTLab), is an SPT type Hall thruster with a 40 mm discharge channel. HK40 was initially designed to operate with SmCo permanent magnets. To optimize the magnetic field topology, the permanent magnets were replaced with iron-core electromagnets. The thruster is operated with different magnetic coil currents to observe the changes in discharge characteristics. Magnetic field topology of the thruster is examined to determine the proper location of a LaB6 hollow cathode, which is also designed and built at BUSTLab. External magnetic field topology of a Hall thruster has an important characteristic called magnetic field separatrix defining the boundary between closed magnetic surfaces and open magnetic field lines. To investigate the effects of the separatrix surfaces, the location of the cathode is changed in-situ with respect to the Hall thruster with a 2-D translational stage in two different grounding configurations, one connecting the vacuum chamber to the same ground with the power supplies, and the other with the power supplies connected to a common floating ground. We show that the influence of the external magnetic field strength on the thruster efficiency can be predicted from the electron current coming from the cathode emitter surface. We also show that the cathode to ground voltage provides a way to estimate the efficiency with respect to the cathode placement. The mechanisms and the efficiency values of two setups are compared to explain the ground and the space operations.

I.   Introduction

Electric propulsion systems are increasingly being employed in satellites and spacecraft as alternatives to chemical thrusters due to their lower propellant consumption and resulting cost savings.[1] Hall-effect thrusters (HETs) are a class of electric propulsion devices. In Hall effect thrusters, electric and magnetic fields are used to create a plasma and to expel the ions at high velocities to produce thrust. Even though the imposed magnetic field affects both the electrons and the ions, the ions move mostly unaffected by the magnetic field due to their higher mass, and are accelerated by the applied electric field. There are three types of electron motion in Hall effect thrusters: (i) electron motion along the local magnetic field lines into the channel, (ii) closed drift, $\mathbf{E} \times \mathbf{B}$, motion to distribute electrons around the channel, (iii) cross-field (transverse) electron motion towards the anode.[2]

The paths of electrons are illustrated in Figure 1. The $\mathbf{E} \times \mathbf{B}$ drift velocity is E/B in magnitude and occurs along the channel circumference contributing to the Hall current. The maximum magnetic field strength is

---

*Graduate Student, Department of Mechanical Engineering, Bogazici University.
†Graduate Student, Department of Mechanical Engineering, Bogazici University.
‡Associate Professor, Department of Mechanical Engineering, Bogazici University.
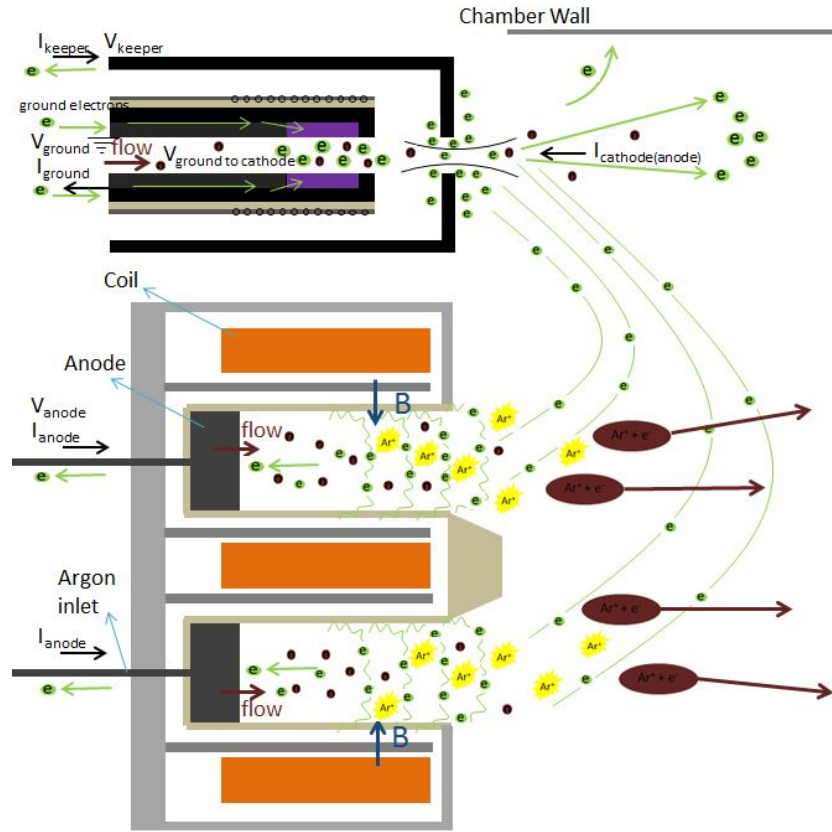§Associate Professor, Department of Engineering Physics, Istanbul Medeniyet University

American Institute of Aeronautics and Astronautics

Figure 1: Schematic of the paths of electrons with ionization

observed in this region where the Hall current exists.[2] Electrons are trapped by magnetic field lines and their cyclotron frequency, $\omega_e = qB/m$, is much higher than that of the ions. Furthermore, the cyclotron frequency of electrons is much greater in comparison to the collisional frequency, $\omega_e >> \nu_e$.[3] In $\mathbf{E} \times \mathbf{B}$ drift region, the Hall parameter, β, is defined as:

$$\beta = \frac{\omega_e}{\nu} = \frac{eB}{m_e \nu} \tag{1}$$

where ν is the electron-heavy particle collision frequency. Since the electrons are well magnetized, the electron Hall parameter is much larger than unity in Hall thrusters.

Cross-field motion is accomplished by electron mobility.[2] The electron momentum collision frequency is defined as:

$$\nu_m = \nu_{ei} + \nu_{en} \tag{2}$$

where ν_{ei} is the electron ion collision frequency and ν_{en} is the electron neutral collision frequency.

However, this equation is not sufficient to explain the cross-field motion of electrons and it is an underestimation for electron current towards the anode according to experimental results.[4]

Morozov included a wall collision frequency term, ν_w, to get higher cross-field transport term.[5] The final addition is the Bohm diffusion term, ν_B. This term is proposed to be coming from instabilities of $\mathbf{E} \times \mathbf{B}$ drift motion because of the Hall current.[4] This concept was studied first by Bohm, Burhop and Massey in 1946.[6] Experimental and numerical studies confirmed that cross-field mobility is highly dominated by Bohm diffusion given by Eq. 3. In this equation the the multiplication factor of 16 is commonly used to match the experimental data.[7]

$$\nu_B = 16\omega_e \tag{3}$$

American Institute of Aeronautics and Astronautics

Thus, the total collision frequency becomes:

$$\nu_m = \nu_{ei} + \nu_{en} + \nu_w + \nu_B \tag{4}$$

Hall parameter, β, and electric conductivity, σ, provide a way to explain the relation between electric field and magnetic field in Hall effect thrusters.

The current density is obtained from the relation:

$$J = \sigma E \tag{5}$$

Conductivity has components in all directions which are all proportional to $1/(1 + \beta^2)$.[8] The current density in the longitudinal direction has relationship:

$$J_z \sim \frac{E}{1 + \beta^2} \tag{6}$$

If the magnetic field strength is high in a region, then the Hall parameter is large, and the current density is low in this region. According to Eq. 5, conductivity and current density are affected by the electric field in a similar manner. Therefore, σ_z would have a proportionality relationship:

$$\sigma_z \sim \frac{1}{\beta^2} \tag{7}$$

According to Eq.7, in the strongest magnetic field region, electron current flow is restricted because electrons are trapped in magnetic field lines. On the other hand, for large ω_e the Hall parameter is large. Electrons follow the magnetic field lines by experiencing cyclotron motion. In the acceleration region, electrical conductivity is low but electric field reaches a maximum value. Electron temperature and plasma potential gradients along magnetic field lines are low. Therefore, the lines are considered as equipotential.[9] As a result, electrons ionize the neutrals in the channel and ions could be attracted to the thruster exit due to low potential at thruster exit.

For the operation of the thruster in optimum conditions, the topology of the magnetic field is an important design parameter. In this study, the magnetic field characteristics of HK40 Hall effect thruster is assessed by considering the location of the electron source which is the LaB_6 insert inside the hollow cathode and the separatrix surfaces formed by the external magnetic field of the thruster. Thruster efficiency mechanisms are investigated by measuring ground current for the grounded setup (section IV.A), and cathode to ground voltage for the floating setup (section IV.B). The vacuum tank effects and the space operation are discussed.

Figure 2: HK40 Hall effect thruster with BUSTlab LaB_6 hollow cathode

II.   HK40 Hall Effect Thruster

HK40, designed and built at BUSTLab, is an SPT type Hall thruster with a dielectric channel outer diameter of 40 mm. In its original design, the thruster had 1/2 $inch$ diameter and 1 $inch$ long cylindrical Samarium-Cobalt permanent magnets; four outer and one inner. Recently, these permanent magnets were replaced with iron-core electromagnets of the same physical size. A rendering of the 3D technical drawing and a side view picture of HK40 with BUSTLab LaB_6 hollow cathode in operation are shown in Figure 2.

External magnetic field topology of a Hall effect thruster has an important characteristic called magnetic field separatrix that signifies the surface which forms the boundary between closed magnetic surfaces and open field lines. Inside the separatrix, magnetic field lines capture electrons near the discharge region and along the beam while outside the separatrix, the magnetic field lines orient electrons away from the beam.[13] In this study, location of the cathode with respect to the separatrix surfaces are investigated in-situ by moving the cathode with a 2-D translation stage.

III.   BUSTLab Hollow Cathode

Electron sources, such as hollow cathodes, are essential parts of the electric propulsion systems ionization and neutralization processes. For Hall thrusters, the cathode electrons ionize the neutral gas in the chamber and neutralize the ion beam exiting the thruster.
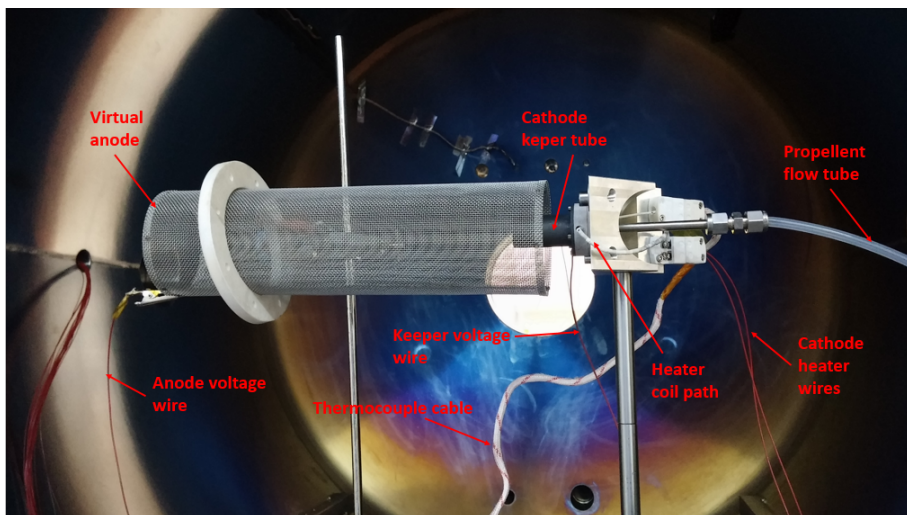

Figure 3: LaB_6 hollow cathode test setup for current extraction with a virtual anode

The prototype hollow cathode, designed and built at BUSTLab, has a 6 mm outer diameter 48 mm long graphite cathode tube. It utilizes a 2 mm ID, 4 mm OD LaB_6 tube of 10 mm length as the thermionic emission material. The insert region of the cathode is heated using a heater assembly that utilizes 0.25 mm diameter tantalum wire that is wrapped around a high temperature machinable ceramic (shapal) tube with external helical grooves. A specially designed coaxial graphite part is used providing current to the heating wire, and alumina parts are used for electrical and thermal insulation of the heater wire.

BUSTLab hollow cathode characteristics were determined by conducting measurements using a virtual anode. The setup for the cathode tests with a virtual anode is shown in Figure 3. By operating the cathode in this setup, virtual anode current and voltage values are obtained for different mass flow rates and keeper current values. According to these tests, the suitable cathode mass flow rate is determined to be 2.2 $sccm$ for Argon propellant.

The source of the electrons that leave the cathode, thus providing the cathode current, is the LaB_6 insert located inside the cathode tube. As seen in Figure 4, the insert is at ground potential. As LaB_6 insert emits electrons, it would start extracting electrons from ground. In the experiments, the electrons extracted from the ground are measured and considered as the cathode current. The cathode current is measured with a multimeter connected to the heater return wire. The cathode is isolated from the ground inside the

American Institute of Aeronautics and Astronautics

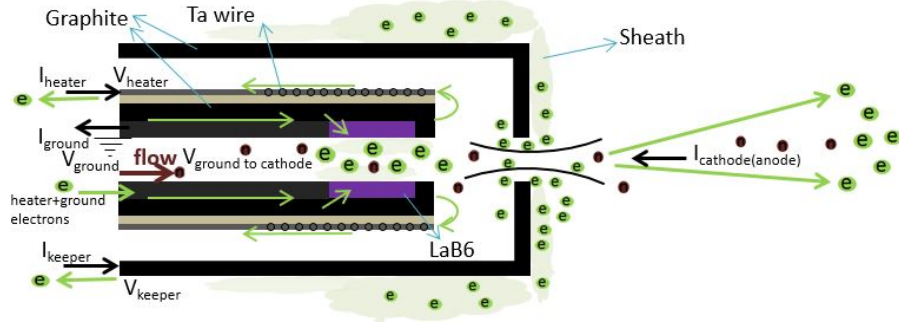vacuum tank so that it attracts all the electrons from the ground outside the tank to be measured with the multimeter.

Figure 4: Electron extraction from LaB_6 emitter surface

IV. Electrical Circuits for the Thruster-Cathode System

In order to illustrate the electrical circuits of the thruster-cathode system for two different setups, representative schematics are created as shown in Figures 5 and 6.

A. Grounded setup

In the first setup the power sources, which provide the anode and keeper voltages, are grounded to the vacuum chamber (V_g). Cathode is also grounded through a multimeter, which measures the cathode to ground current (I_g).
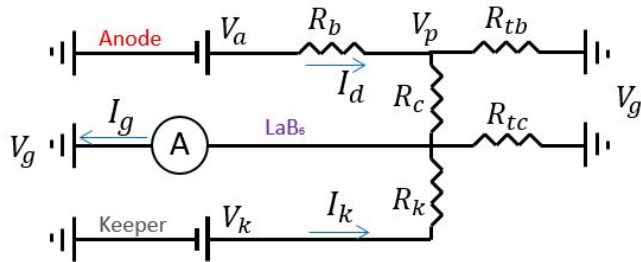

Figure 5: Electrical circuit for the thruster-cathode system for the grounded setup

The anode and the cathode can be characterized as a closed circuit where R_b, R_c, and R_k are the resistances between plasma and anode, plasma and cathode (LaB_6 insert), and keeper and cathode (LaB_6 insert), respectively. R_k is the resistance between the cathode insert and the keeper. R_b is created by the magnetic field topology in the discharge channel and is proportional to the square of the Hall parameter as in the Eq.7. Therefore R_b increases by the increased strength of the magnetic field resulting in more ionization in the channel. The magnitude of the radial component of the magnetic field should not be too high to prevent the electron current towards the anode. R_c depends on the placement of the cathode as well as the external magnetic field topology of the thruster. R_c is the main concern of this study. In the current study, the movement of the hollow cathode using a 2-D translation stage affects the value of R_c.

Since the ground tests are conducted inside the vacuum chamber, R_{tb} and R_{tc} terms are added to the system, which represents the resistance between the thruster plume and vacuum chamber wall, and the resistance between the cathode and the vacuum chamber wall, respectively.

American Institute of Aeronautics and Astronautics

B.   Floating setup

In the floating setup, the negative ends of the power sources of the anode and keeper, and the return wire of the heater, which is connected to the insert material, are all connected at a floating common point (called the *common ground*). Common ground and the ground of the vacuum chamber are connected through a multimeter, which measures the voltage (V_{cg}) between the floating common ground voltage and ground voltage. This setup represents the electrical circuit of a thruster on a spacecraft.
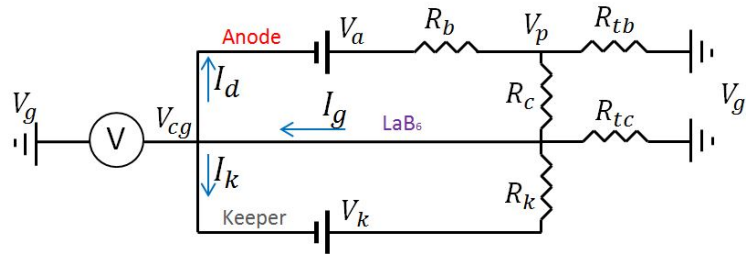

Figure 6: Electrical circuit for the thruster-cathode system for floating setup

In this setup, cathode current (I_g) is equal to the sum of the keeper current (I_k) and discharge current (I_d). In this configuration, total neutralization of the ion beam leaving the thruster is achieved.
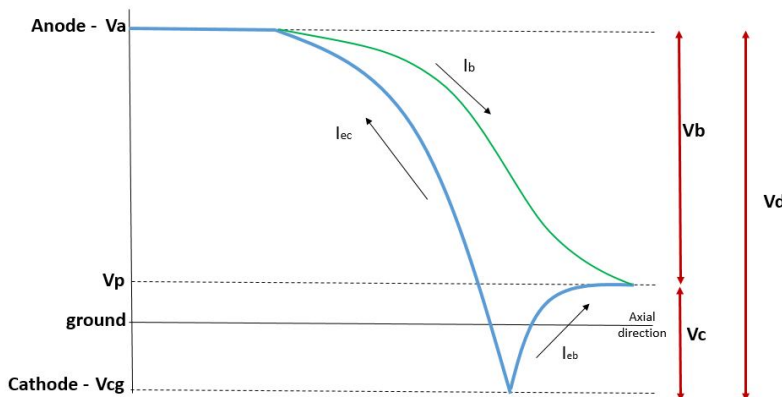

Figure 7: Hall thruster voltage schematic

The potential difference between the anode and the cathode generates the discharge voltage (V_d) as can be seen in Figure 7. In the grounded setup, cathode voltage (V_{cg}) is zero, therefore anode voltage (V_a) is equal to the discharge voltage and read from the power source. In the floating setup, cathode voltage (V_{cg}) is not zero, therefore the potential difference that is generated by the power source is the discharge voltage which is equal to the difference between the anode voltage (V_a) and cathode voltage (V_{cg}).

Plasma potential (V_p) is measured in the thruster plume and defined as the voltage at the thruster exit where the ion acceleration is completed. The accelerated ions fall through a potential (V_b), that corresponds to the potential difference between the anode voltage and the plasma potential. Cathode coupling voltage (V_c) is the voltage between the plume plasma potential and the cathode voltage.

American Institute of Aeronautics and Astronautics

V.   Theoretical Estimation of Thruster Efficiency

A.   Calculating efficiency from the ground current

The ions are accelerated from the location of their creation inside the discharge chamber towards the downstream plume region. The plume plasma potential depends on the electron current supplied from the cathode, magnetic field topology, the placement of the cathode and the discharge characteristics. Even though the ions are created at a region that has slightly less potential than the anode potential, it can be estimated that the beam power is:

$$P_b = I_b(V_a - V_p) \tag{8}$$

Beam current (I_b) is calculated from the difference between the discharge current (I_d) and the electron current emitted from the cathode (I_{ec}) as in Eq.9.[4] The discharge current is formed by incoming electrons from the cathode and by the ionization of the neutrals:

$$I_d = I_{ec} + I_b \tag{9}$$

where I_{ec}, the cathode electrons, is measured from the ground current. There are equal number of electrons and ions in the plasma discharge after ionization as seen from Eq. 10:

$$I_b = I_{ei} \tag{10}$$

where I_{ei} is the electrons created after ionization. The created ions are expelled towards the exit while electrons flow towards the anode as depicted in Figure 1. The thrust is calculated as:

$$T = \frac{I_b m_i}{e} \sqrt{\frac{2eV_b}{m_i}} \tag{11}$$

and the efficiency becomes:

$$\eta_T = \frac{1}{2} \frac{T^2}{\dot{m}_t P_t} \tag{12}$$

where $\dot{m}_t$ is the sum of mass flow rates to the anode and the cathode, and P_t is the total power which includes the power to anode, keeper and magnetic coils.[10]

With an increase in magnetic field strength, anode voltage becomes higher for a constant discharge (anode) current. With constant discharge current, ground current (current from ground to the cathode) decreases, meaning that the electron current extracted from the cathode decreases as will be explained in Section VII.

B.   Calculating efficiency from cathode to ground voltage

For this setup, the discharge current is equal to the cathode current.

$$I_d = I_{cathode} \tag{13}$$

also the cathode electrons ionize the neutrals I_{ec} and neutralize the beam ions I_{eb}:

$$I_{cathode} = I_{ec} + I_{eb} \tag{14}$$

The voltage that accelerates the ions is calculated as the difference between the applied anode voltage and the cathode coupling voltage as in Figure 7.

$$V_b = V_d - V_c \tag{15}$$

Thrust is defined as:

$$T = \dot{m} v_{avg} \tag{16}$$

where $\dot{m}$ is the ionized propellant mass flow rate and v_{avg} is the average axial exit velocity of ions given by:

$$v_{avg} = a \sqrt{\frac{2e(V_d - V_c)}{m_i}} \tag{17}$$

American Institute of Aeronautics and Astronautics

where m_i represents ion mass, a is a constant coming from the divergence losses calculated with the divergence half angle, $cos(\theta)$, and e is the electron charge.[11] Argon ions are assumed to be only singly ionized.

Thruster efficiency is calculated as in Eq.12 by calculating the mass flow rate of the ionized gas from the beam current:

$$\eta_T = \frac{a^2 e\dot{m}(V_d - V_c)}{m_i(I_d V_d + P_{magnet} + P_{cathode})} \tag{18}$$

where I_d is the current supplied to the anode.

In the conducted experiments, by measuring the ground current the beam current is calculated from the cathode current. Regarding the beam current, the ionization ratio of the propellant is calculated to be in the range of $75 - 80\%$ when an Argon flow rate of 18 $sccm$ is supplied to the anode. This ratio is used for the calculation of thrust using Eq.16. The loss caused by the beam divergence are estimated from the visual observation of the thruster operation. The divergence angle was taken to be 40 degrees. The efficiency value calculated with this angle and named as *corrected efficiency*.

VI. Experimental Setup for the Cathode Placement Tests
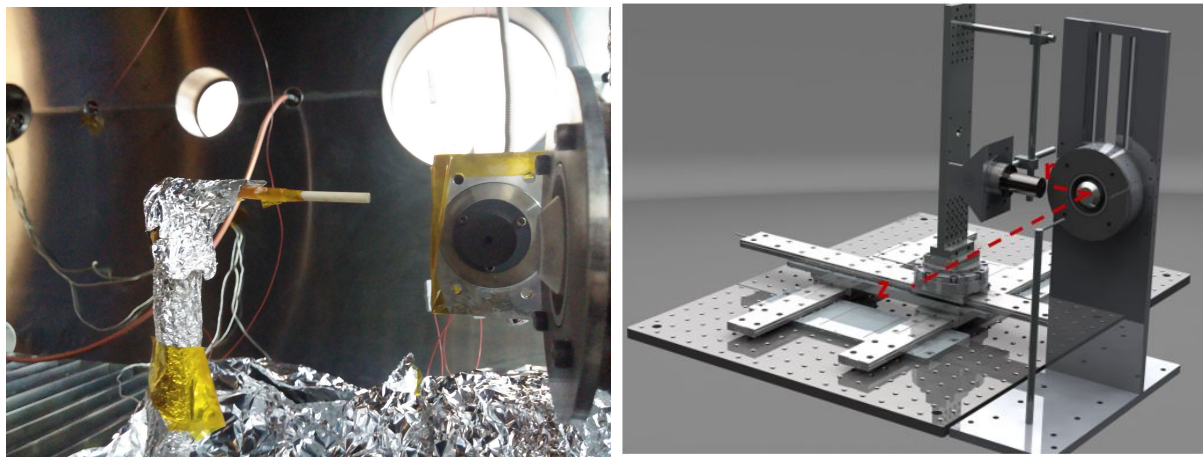

Figure 8: a) Side view of the HK40 and BUSTLab hollow cathode inside the chamber (with a Langmuir probe in front of the thruster) b) 3D rendering of the experimental setup (with axial and radial directions indicated)

HK40 Hall thruster tests were conducted inside the BUSTLab vacuum chamber which is a 1.5 m diameter 2.7 m long cylindrical tank. Rough pumping is achieved by a combination of Oerlikon rotary wane pump and roots blower. A pressure on the order of 3×10^{-3} $Torr$ is obtained by the mechanical pump system. As the next step, approximately 10^{-7} $Torr$ is achieved with the help of two cryopumps.

In order to conduct the experiments, various gas and electrical feedthroughs have been used to provide gas flow and power to inside the chamber. A picture of the HK40 Hall thruster placed inside the BUSTLab vacuum chamber is shown in Figure 8a. The cathode is moved by a 2D translational stage. The origin is decided as the center of the Boron Nitride channel cup at the exit plane of the thruster. The directions used in the test are illustrated on a rendering of the 3D technical drawing of the experimental setup as shown in Figure 8b.

Before the tests, the magnetic field topology of the thruster for different currents to inner and outer electromagnets are determined by a transverse Hall probe. In these measurements, conducted outside the vacuum chamber, two different power sources are used for supplying desired currents to inner and outer magnet coils. The magnetic flux density values are measured by a Lakeshore DSP 455 Gaussmeter operated with LabVIEW on computer.

During the experiments, the discharge current is kept constant 1.2 A for all the tests. Two different power supplies were used to to supply the inner magnet coils with a current of 1.7 A, and the outer magnet coils
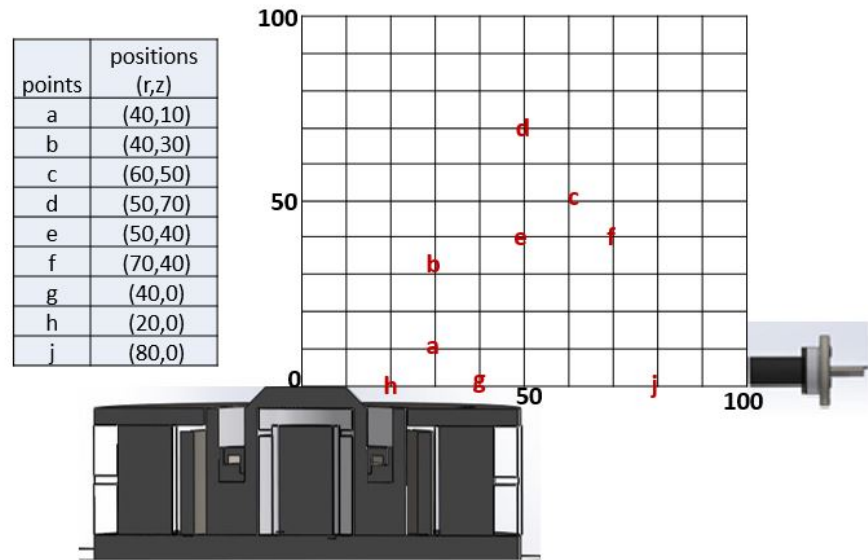
points	positions (r,z)
a	(40,10)
b	(40,30)
c	(60,50)
d	(50,70)
e	(50,40)
f	(70,40)
g	(40,0)
h	(20,0)
j	(80,0)

Figure 9: Test points in 2D plane for the grounded setup (inner coil = 1.7 A, outer coils = 2 A)

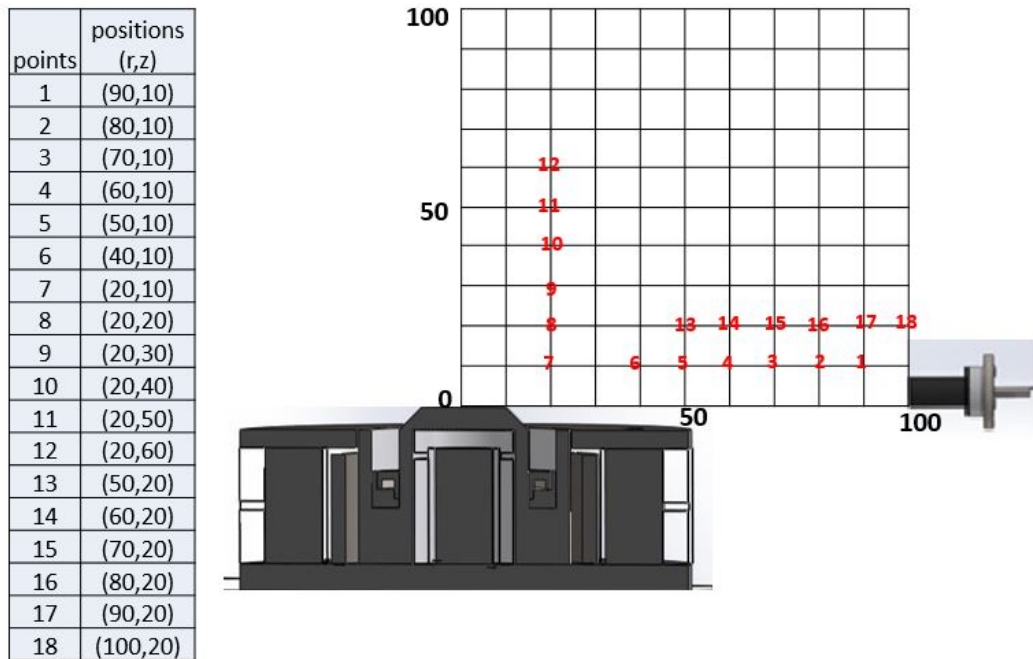| points	positions (r,z)
1	(90,10)
2	(80,10)
3	(70,10)
4	(60,10)
5	(50,10)
6	(40,10)
7	(20,10)
8	(20,20)
9	(20,30)
10	(20,40)
11	(20,50)
12	(20,60)
13	(50,20)
14	(60,20)
15	(70,20)
16	(80,20)
17	(90,20)
18	(100,20)

Figure 10: Test points in 2D plane for the floating setup (inner coil = 1 A, outer coils = 1.2 A)

with a current of 2.0 A. These magnet current values are determined as the optimum operation currents for the grounded tests . The Hall probe results are compared with COMSOL modeling of the thruster magnetic field topology and the model is optimized after the measurements. According to the magnetic topology model, for the stated inner and outer magnet current values the maximum magnetic field strength in the channel is 360 G. For this setup, the efficiency is predicted using Eq.12 regarding the ground current. The power supplies are grounded and the current extracted from the ground is measured by serially connecting

American Institute of Aeronautics and Astronautics

a multimeter between the heater return wire and the ground. The locations at which data were taken are illustrated in Figure 9.

For the tests conducted with the floating setup to measure cathode to ground voltage, the optimum magnetic field was obtained by supplying 1 A to the inner coil and 1.2 A to the outer coils. For these current values the maximum magnetic field strength was determined to be 220 G. HK40 and hollow cathode were operated in the vacuum chamber. The discharge characteristics and cathode-to-ground voltage were measured in-situ while changing the relative location of the cathode with respect to the HK40. Efficiency is calculated using Eq.18 by measuring the cathode to ground voltage. The locations at which data were taken for the floating setup are illustrated in Figure 10. During these tests, all the electronic parts are connected to a common ground as described in section IV.B.

The plume plasma characteristics were investigated by measuring electron number density, electron temperature, and plasma potential using a single Langmuir probe. The probe used in these measurements have a 1 mm diameter molybdenum rod inside a single hole alumina tube of 3.2 mm OD. A Keithley 2410 sourcemeter is used for biasing the probe electrode and collecting current.

To observe the separatrix surface, a finite element model of the HK40 Hall effect thruster was constructed over a 2D domain which was obtained from the cross-section cut of the 3D CAD drawing of the thruster. The numerical simulations were done using COMSOL finite element software. The cross-section plane passes through the center of the thruster and the centers of electromagnets for the latest design. The colored contours show the z-component of the vector potential with values very close to zero, which stands for the separatrix surface.

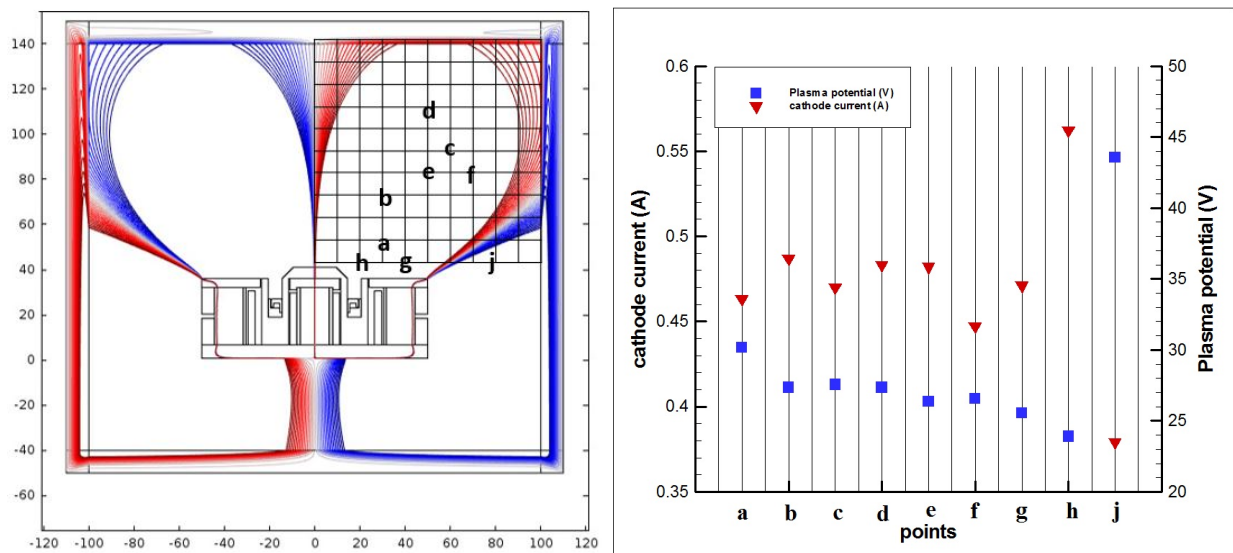# VII.   Results and Discussions

Figure 11: a) Test points with respect to separatrix surfaces (inner coil = 1.7 A, outer coils = 2 A) b) Changes in electron current and plasma potential at specified points (inner coil = 1.7 A, outer coils = 2 A)

The tests were conducted with two different setups as mentioned earlier. The data points were selected considering the separatrix surfaces. For the grounded setup, as the cathode is moved away from the thruster radially, the cathode current decreases sharply after the separatrix. The reason for that could be the increased resistance (R_c) created by the magnetic field lines in front of the cathode. When the discharge current is constant as 1.2 A, the ionization in the discharge chamber should be higher if the cathode is outside the separatrix to satisfy the condition in Eq.9. At point j, plasma potential is measured by the Langmuir probe to be 43 V with less electron supplied from the cathode, while the potential is 23 V at point h in Figure 11. However, the anode voltage increases as the cathode is moved from point h to point j due to the resistance caused by the presence of magnetic field. The increase in the anode voltage is larger than the increase in

American Institute of Aeronautics and Astronautics

the plasma potential. Therefore, the beam voltage is higher at point j relative to point h. The other points inside the separatrix have close values for the cathode current and the plasma potential.
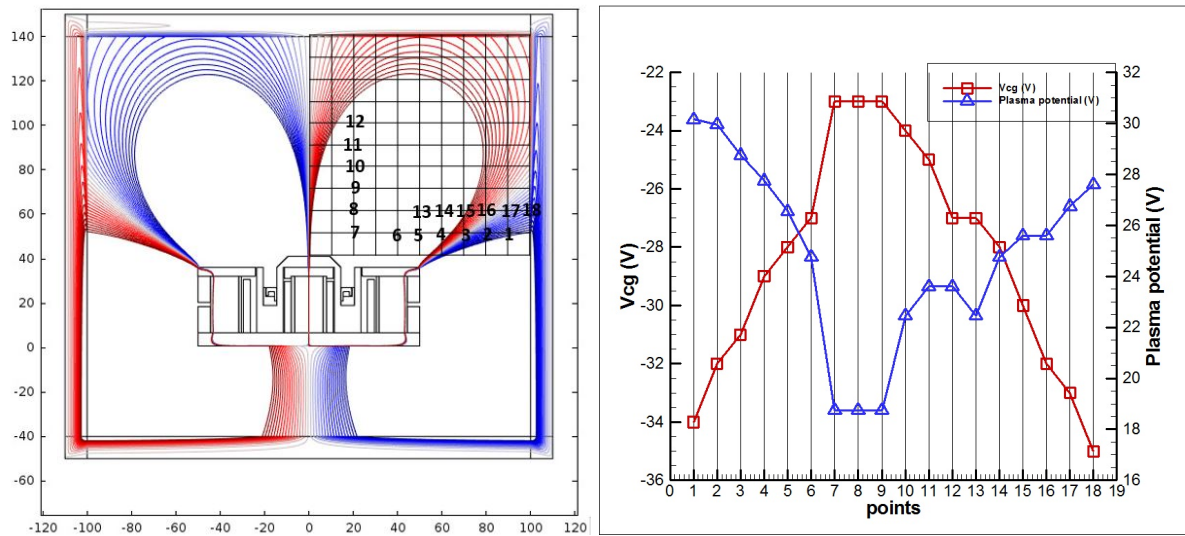

Figure 12: a) Test points with respect to separatrix surfaces (inner coil = 1 A, outer coils = 1.2 A) b) Cathode to ground voltage, V_{cg}, and plasma potential, V_p, at specified points (inner coil = 1 A, outer coils = 1.2 A)

For the floating setup where the negative leads of all the supplies are connected at a common floating ground, the cathode is moved radially and axially by considering separatrix surfaces as shown in Figure 12. For the radial movement of the cathode, the cathode to ground voltage values show a linear variation. As the cathode is located closer to the discharge channel, the cathode to ground voltage (V_{cg}) is smaller in magnitude.

As the cathode is moved axially from point 7 to point 12, plasma and cathode to ground voltages are investigated. Points 7, 8 and 9 have the same V_p and V_{cg} values, hence it was observed that cathode position does not affect the plume plasma, but different discharge voltages are measured at these positions. For points from 7 to 12, the cathode is placed almost inside the plume. Therefore, R_c is small, thus changing the cathode position affects R_b. In order to attract the same amount of the discharge current, the anode voltage becomes higher to overcome the resistance cause by the magnetic field, R_b. It can be claimed that both the radial and axial distance of the cathode directly affects the discharge voltage.

Thrust and efficiency values of the tests are compared in Figure 13 for the two different setups discussed earlier. For the grounded setup tests, thrust and efficiency values are calculated with Eqns 11 and 12. The point j has the highest thrust and efficiency values, with less cathode current and higher beam current. For the floating setup, Eqns 16 and 18 are used. Evaluated values for points 4 and 15 show jumps in the set of data. These two points are almost on the separatrix surfaces as can be seen in Figure 12. Similarly point 10 and 11 also show values that are outside of the expected trend lines, but the reason for this observation is not clear. Apart from these observations of points where small deviations were observed, the calculated thrust values are very close to each other and are within 12.1 to 12.4 mN range. The efficiency values show variations with respect to the cathode position. The efficiency is lower for cases where the cathode is located outside of the separatrix as in the cases of points 1 and 18. Point 9 seems to be the optimum cathode location for both thrust and efficiency.

Since different efficiency calculations are made, there could be some discrepancies in the presented comparisons. Especially, predicting the beam current without complete neutralization of the ion beam for the grounded setup, and the uncertainty in beam divergence angle for the floating setup can result in an overestimation of the calculated thrust and efficiency values. Considering the obtained results, the floating setup provides higher thrust and efficiency values. The floating setup would also better correspond to an in-space operation of the thruster cathode system. Also, the optimum magnetic coil currents, thus the magnetic field strengths and topology, are different for the two setups. According to the results, the floating setup provides

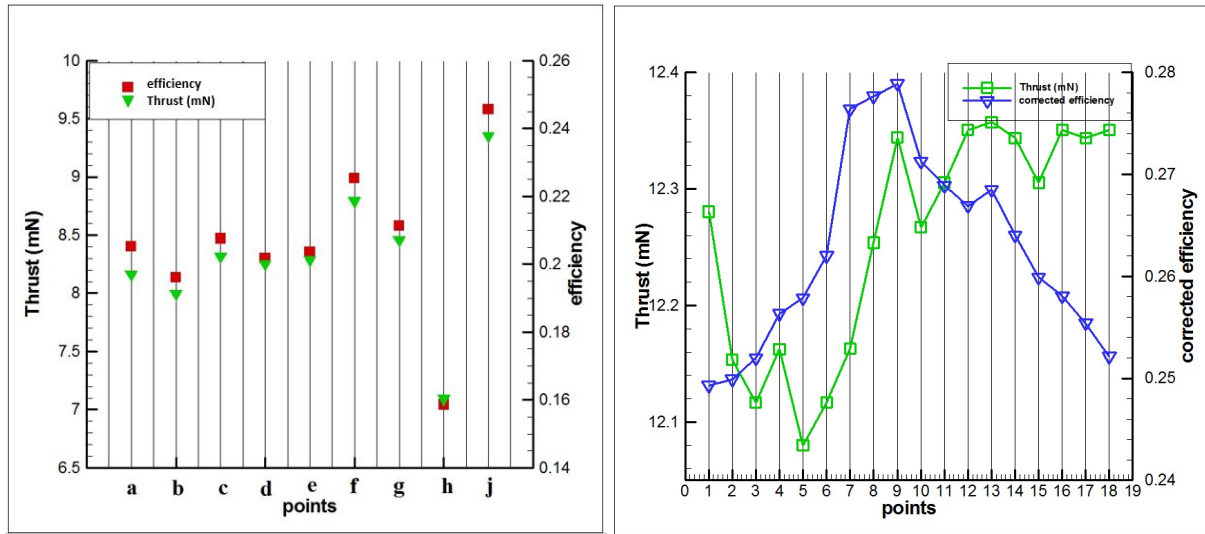American Institute of Aeronautics and Astronautics

Figure 13: a) Efficiency and thrust values at specified points (inner coil = 1.7 A, outer coils = 2 A) b) Thrust and efficiency at specified points (inner coil = 1 A, outer coils = 1.2 A)

a more efficient operation condition for HK40 as this setup requires less power for the coils, and requiring only 220 G of maximum magnetic field strength in the discharge channel region.

Magnetic field topology shapes the equipotential surfaces from the anode to the cathode. High Hall parameter which increases in the high magnetic field region causes the increase of the beam resistance (R_b) in the high magnetic field region of the discharge chamber (the acceleration region), thus the voltage drop between the anode and cathode voltages is concentrated in the acceleration region. The trapped electrons cause a decrease in voltages by helping the ions to move towards the exit. The electrons expelled from the cathode are just a starter for the ionization process. For Hall thrusters, ionization cost is the main loss mechanism because to accelerate the ions the propellant should be ionized efficiently first. Then, the ions are accelerated by Lorentz Force that is created by the electric field resulting from the voltage drop in the acceleration region.

For the constant discharge current of 1.2 A and the anode propellant mass flow rate of 18 $sccm$ as in our system, less cathode current means more efficient system, because the beam current constructed by the ions is the difference between the cathode (electron) current and the discharge current (Eq. 9). The thrust depends on the voltage difference between the anode and the plasma formed between the anode and the cathode. The cathode electrons play a role to reduce the plasma potential causing the acceleration of the ions falling from the anode voltage. Therefore, the cathode should continue to emit electrons to keep the plasma potential at a desired level.

For the case of the grounded setup, the cathode emits less electrons when placed outside the separatrix. The cathode potential is near zero as could be seen from Figure 5. The cathode current is relatively independent of the discharge current. Therefore, the cathode current is dominated by the magnetic field and the location of the separatrix. For this setup, the tank walls and the cathode are at potentials very close to the ground potential. An electron beam towards the tank is not observed. All the electrons expelled from the cathode flow towards the thruster. This is the reason why the grounded setup is useful for eliminating the effects of the tank and for observing the cathode operation.

The floating setup is an example of the space operation. However, the tank walls affect the electron pathways during the experiments. The cathode current should be equal to the discharge current. Therefore, the cathode emits the same amount of electrons regardless of the magnetic field separatrix and the position of the cathode. However, as the cathode is moved away from the thruster, the cathode coupling voltage becomes large in magnitude and the electron density inside should be larger. Electrons continue to collide with neutrals inside the cathode creating more electrons and provide self-heating. This condition is also a loss mechanism as the electrons get hotter inside the cathode. For this setup, since the cathode voltage and the ground voltage are different, electrons exiting from the keeper follow different paths with respect to the

American Institute of Aeronautics and Astronautics

separatrix surface as observed during experiments. Although the same amount of electrons are expelled, some of them go to the tank walls. When the cathode is moved outside of the separatrix surfaced, R_c increases and the cathode and plasma voltages arrange themselves to a new value. As in Figure 6, V_{cg} becomes more negative and V_p becomes larger to supply the same I_d with the increased resistance. When the cathode has higher negative voltage, the chamber walls attract more electrons. However, in space, R_{tb} and R_{tc} resistances do not exist.

In a study conducted by Frieman et al., the authors claim that separatrix has no effect on the cathode coupling voltage.[12] The authors propose that due to the loss of magnetization in regions away from the thruster, electron current collection pathways towards the thruster body and the facility walls change. For the region very close to the thruster exit, the path is the thruster body while for the regions away from the thruster, the path is towards the walls. Because of the recombination pathways, it is suggested that on ground and in space operations are different. However, the measured thrust and the discharge current do not change significantly by moving cathode in their study. It is asserted that the cathode placement does not change ionization process in discharge channel.[12] However, Sommerville claims that separatrix has an effect on the cathode coupling voltage and efficiency.[13] According to our results, at the floating setup which represents the space application, the cathode to ground voltage is not affected by the separatrix but the cathode to ground voltage is a linear function of the radial distance from the thruster center axis irrespective of which side of the separatrix surface the cathode is located.

VIII.   Conclusion

In this study, the operation of HK40 Hall effect thruster is studied for various cathode locations using two different grounding configurations. In the first setup, the power supplies are all grounded and the cathode is at near the ground potential. The cathode current is measured to determine the optimum location of the cathode. It was observed that the magnetic field sepratrix has an effect on the cathode operation according to evaluated thrust and efficiency values. In the second setup where a floating ground is used, the cathode potential is below the ground potential. It was observed that in this wiring configuration, as the cathode location is changed the cathode current remains constant while the cathode to ground voltage changes. The increase in the cathode to ground voltage, V_{cg}, is explained by using a electrical circuit analogy where different parts of the thruster cathode system are represented by appropriate resistances. For the floating setup, the separatrix has no effect on thruster operation; however, vacuum tank, which is at the ground potential, attracts part of electrons exiting the cathode. For this setup, the cathode should be placed inside the separatrix surfaces. The effects of the tank walls should be studied further in future experiments.

Acknowledgements

References

[1]Martinez-Sanchez, M. and Pollard, J.E., *Spacecraft Electric Propulsion-An Overview*, Journal of Propulsion and Power, Vol. 14, No. 5, 1998, pp. 688699.

[2]Xu, K. G. and Walker, M. L., *Effect of External Cathode Azimuthal Position on Hall-Effect Thruster Plume and Diagnostics*, Journal of Propulsion and Power, Vol. 30, No. 2, 2014, pp. 506-513.

[3]Ahedo, E. and Gallardo, J., *Low Power Hall Thrusters: Physics, Technical Limitations and Design*, Micropropulsion Workshop, Lerici, Italy, May 2002.

[4]Goebel, D. M. and Katz, I., *Fundamentals of Electric Propulsion: Hall Thrusters*, JPL Space Science and Technology Series, New York, USA, 2008.

[5]Morozov, A. I., Esipchuck, Y., Kapulkin, A. M., Nevrovskii, V. A. and Smirnov, V. A., *Effect of the Magnetic Field on a Closed Electron Drift Accelerator*, Soviet Physics Technical Physics, vol. 17, no. 3, 1972.

[6]Chen, F. F., *Introduction to Plasma Physics and Controlled Fusion*, Volume 1:Plasma Physics, Plenum Press, New York, USA, 1984.

[7]Fossum, E. C. and King, L. B., *Design and Construction of an Electron Trap for Studying Cross-Field Mobility in Hall Thrusters*, 43rd Joint Propulsion Conference, Cincinnati, OH, USA, July 2007, AIAA 2007-5207.

American Institute of Aeronautics and Astronautics

[8]Petit, J. P. *Cancellation of the Velikhov Instability by Magnetic Confinement*, 8th International Conference on MHD Electrical Power Generation, Moscow, USSR, 12-18 September 1983.

[9]Kim, V., *Main Physical Features and Processes Determining the Performance of Stationary Plasma Thrusters*, Journal of Propulsion and Power, Vol. 14, No. 5, 1998, pp. 736-743.

[10]Jameson, K. K., Goebel, D. M., Hofer, R. R. and Watkins, R. M., *Cathode Coupling in Hall Thrusters*, 30th International Electric Propulsion Conference, Florence, Italy September 2007, IEPC-2007-278.

[11]Sommerville, J. D. and King, L. B., *Effect of Cathode Position on Hall-Effect Thruster Performance and Cathode Coupling Voltage*, 43rd Joint Propulsion Conference, Cincinnati, OH, USA, July 2007, AIAA-2007-5174.

[12]Frieman, J. D., Walker, J. A., Walker, M. L., Khayms, V., and King, D. Q., *Electrical Facility Effects on Hall Thruster Cathode Coupling: Performance and Plume Properties*, Journal of Propulsion and Power, 2015, pp. 1-14.

[13]Sommerville, J.D., *Hall-Effect Thruster Cathode Coupling: The Effect of Cathode Position and Magnetic Field Topology*, Ph.D. Thesis, Michigan Technological University, Houghton, MI, USA, 2009.

American Institute of Aeronautics and Astronautics